A collinear angle-resolved photoelectron spectrometer

O. Windelius[a,c], A. Aguilar[b], R.C. Bilodeau[b,d], A.M. Juarez[e], I. Rebolledo-Salgado[e], D.J. Pegg[f], J. Rohlén[c], T. Castel[g], J. Welander[c], D. Hanstorp[c]

[a] *Department of Physics, Chalmers University of Technology, SE-41296 Gothenburg, Sweden*
[b] *Advanced Light Source, Lawrence Berkeley National Laboratory, Berkeley, CA 94720, USA*
[c] *Department of Physics, University of Gothenburg, SE-41296 Gothenburg, Sweden*
[d] *Department of Physics, University of Connecticut, Storrs, CT 06269*
[e] *Instituto de Ciencias Fisicas, Universidad Nacional Autonoma de Mexico, PO Box 48-3, Cuernavaca 62251, Mor. Mexico*
[f] *Department of Physics, University of Tennessee, Knoxville, Tennessee 37996, USA*
[g] *École Nationale Supérieure d'Ingénieurs de Caen, ENSICAEN 6 Boulevard Maréchal Juin 14050 Caen, France*

Abstract

In the present paper we describe a newly designed collinear photoelectron spectrometer for angular distribution measurements. We will henceforth refer to this instrument by the acronym **PEARLS** (**P**hoto**E**lectron **A**ngle-**R**esolved **L**inear **S**pectrometer). The design was motivated by the desire to collect electrons emitted from an extended linear source consisting of collinear photon and ion beams at a synchrotron radiation site. The electrons could be produced in either photoionization or photodetachment events. The primary advantage of a collinear beams geometry is that the effective interaction volume can be made much larger than that obtainable with a crossed beams geometry, which has been used in many earlier photoelectron spectroscopic studies. The present apparatus is capable of collecting electrons over a beam source length of 22 cm. The electrons are detected using Channel Electron Multipliers (CEMs). There are 4 detector planes placed perpendicular to the direction of the beam source, where each plane contains 4 CEMs. The use of all 4 detector planes with a total of 16 CEMs enhances the photoelectron signal, which is important at a synchrotron radiation site where the photon flux is typically low. If photoelectrons of different energies are emitted, the design allows for electrostatic energy analyzers to be placed in front of the CEMs. We have performed a photodetachment experiment to demonstrate the functionality of the **PEARLS** apparatus using a pulsed laser as the photon source. In particular, we have measured the angular distribution of photoelectrons ejected from Ag^- at two different photon energies.

Keywords: Photoelectron spectroscopy; photodetachment; photoionization; angular distributions; synchrotron radiation

1. Introduction

For many years, photoelectron spectroscopy has provided valuable information on the properties of atomic and molecular systems via the processes of photoionization and photodetachment [1, 2, 3]. In the present paper we will focus on the photodetachment of negative ions. The general lack of excited states with allowed dipole transitions prohibits conventional bound-bound state photon absorption spectroscopy. Essentially all information on the structure and dynamics of negative ions has been provided by the bound-free photodetachment process [3, 4, 5].

In photodetachment the energy and angular momentum of a photon is transferred to a negative ion, which subsequently breaks up into a neutral atom and a free electron. The initial energy and angular momentum is conserved and shared in the final state by the residual atom and the free electron. A known fraction of the energy transfer appears as kinetic energy in the free electron. Thus, measurements of photoelectron energies allows one to determine the binding energy of the electron in the negative ion prior to detachment [6, 7]. The angular momentum transfer is manifested in the angular distribution of the detached photoelectrons [8, 9]. The shape of a photoelectron angular distribution is characterized by an asymmetry parameter, β. Measurements of the photon-energy dependence of asymmetry parameters can provide information on the relative amplitudes and phases of the partial waves representing the detached electron in the final state.

Essentially all experimental investigations of photodetachment are accelerator based and have been conducted using mass-selected beams of negative ions that are essentially uni-directional and mono-energetic. Most studies to date have employed conventional lasers as the photon source. Such sources are able to provide photons over a wide range of wavelengths from the infrared to the ultraviolet. Free-electron lasers and synchrotron radiation sources are available for measurements requiring photon energies outside the range of conventional lasers [10, 11]. The interaction geometry used to mate the ion and laser beams is chosen according to the type of experiment under consideration. For example, essentially all photoelectron angular distribution measurements have employed a crossed beams geometry in which a negative ion beam is crossed perpendicularly with a linearly polarized laser beam. Energy- and angle-resolved measurements can be made using various types of electron spectrometers [12, 13]. The well-defined spatial interaction volume allows one to efficiently collect and detect photoelectrons. However, the small interaction volume associated with a crossed beams geometry results in a low rate of production of photoelectrons. Clearly, one could substantially increase the production rate by merging the laser and ion beams in a collinear interaction geometry. This advantage, however, is offset by the difficulty of collecting electrons from a relatively long linear source. The first attempt to solve the problem was made by Hanstorp et al. [14], who surrounded a collinear ion-laser interaction region with a cylindrical graphite tube. A line of holes were drilled along the length of the tube in a direction perpendicular to the axis of the collinear source. Photoelectrons ejected

from the source passed through these holes on their way to a detector. Angular distributions were measured by rotating the polarization vector of the laser [15]. In the present paper we describe a new apparatus, **PEARLS** (**P**hoto**E**lectron **A**ngle-**R**esolved **L**inear **S**pectrometer), designed to study angular distributions of photoelectrons emitted from the collinear interaction of beams of positive or negative ions with a photon beam from a synchrotron radiation source. **PEARLS** was designed to permit angle-resolved measurements without the need to rotate the polarization vector of the synchrotron radiation (a difficult procedure usually leading to a substantial loss of flux). To our knowledge, the only previously reported measurement of an angular distribution involving a collinear source and synchrotron radiation was that of Al Moussalami et al [16, 17]. In this photoionization experiment the ejected electrons were collected from a relatively small volume within the merged beams source. It therefore suffered from a low production rate, similar to that in a crossed beams experiment.

The testing of the functionality of **PEARLS** at a synchrotron radiation facility was impractical due to the high demand for beamtime at such sites. Instead, we conducted offline tests of the ability of **PEARLS** to be used in angular distribution measurements by using lasers as the photon source. The test experiments, which were performed at Gothenburg University, involved the photodetachment of Ag^- and P^-. Negative ions were chosen for the commissioning of **PEARLS** since their small binding energies allow photoelectrons to be produced using visible laser sources available in our laboratory. However, the design will allow angular resolved photoelectron studies of both negative and positive ions of atoms, molecules, clusters as well as larger biomolecules.

2. Photoelectron angular distributions

The differential cross section for photodetachment, $\frac{d\sigma}{d\Omega}$, can be written, under the assumption that the target is unpolarized (as is the case for an ion beam) and within the dipole approximation, as [8]

$$\frac{d\sigma}{d\Omega} = \frac{\sigma}{4\pi}(1 + \beta P_2(\cos\theta)). \tag{1}$$

Here, σ is the total cross section and θ is the angle between the direction of the linear polarization of the photons and the momentum of the outgoing electrons. The angular part of the equation contains $P_2(\cos\theta)$, the second-order Legendre polynomial, and the asymmetry parameter β, which completely describes the angular distribution of the photoelectrons. The asymmetry parameter contains information on the relative amplitudes and phases of the partial waves that represent the free electron in the final state. These waves carry orbital angular momenta that differ from that of the bound electron as a result of absorbing a photon. In the case of an electric dipole transition, the change Δl in orbital angular momentum of the detached electron is $|\Delta l| = 1$. Thus, if an s-orbital electron is detached from a negative ion, the free electron will be represented by a pure p-wave. If, however, a p-orbital electron is detached, it will be represented by a superposition of s- and d-waves. Close to the detachment threshold the d-wave is suppressed due to the centrifugal barrier and so the s-wave dominates.

According to Eq. 1, the number of electrons emitted in any direction is proportional to the angular factor $1 + \beta P_2(\cos\theta)$. Therefore, in principle, the asymmetry parameter β can be determined by comparing the number of counts, C, registered in two orthogonal detectors placed parallel to and perpendicular to the direction of the polarization vector of the photons. However, if the ions are moving, one must consider transformations between the Ion Frame (IF) and the Lab Frame (LF). For example, in order for detached electrons to be emitted and detected in the LF at 90° with respect to the ion beam direction, they must be emitted in a backward direction in the IF (see Fig. 1). The angle, α, between the electron momenta in the two frames of reference is a function of the magnitudes of the ion velocity and the velocities of the electron in the IF and LF. This kinematic effect becomes decreasingly important as the angle θ between the directions of the detector and the polarization vector increases. In the limit of $\theta = 90°$, it vanishes altogether (See Fig. 1b).

One way to compensate for this frame transformation effect is to simulate the photoelectron angular distribution experiment using certain values of β as input, and compare the simulation output with the experimental results. It is reasonable to assume that the LF differential cross section to first order has the approximate form

$$\frac{d\widetilde{\sigma}}{d\Omega} = \frac{\widetilde{\sigma}}{4\pi}(1 + \widetilde{\beta} P_2(\cos\psi)), \tag{2}$$

where $\widetilde{\sigma}, \widetilde{\beta}$ and the angle ψ are measured in the LF. Then, by setting $\psi = 0°$

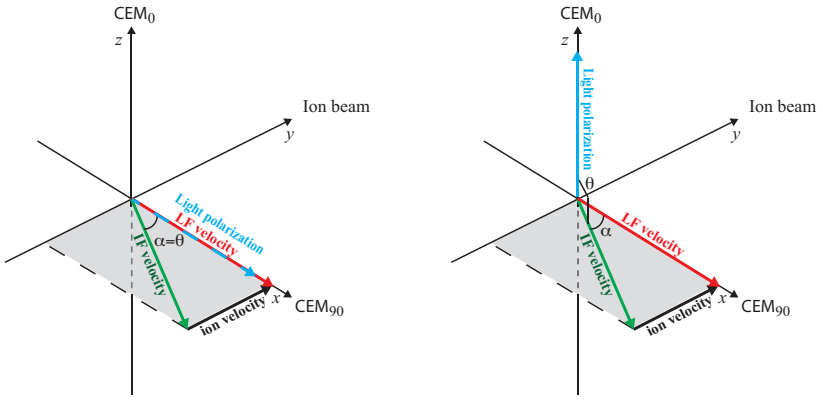

Figure 1: (Color online) For a given ion beam velocity, the kinematic effect produces a difference in emission angle, α, between the electron momentum in the IF and the LF. (a) If the light polarization is along the detection direction, electrons detected in CEM_{90} placed parallel to the polarization vector in the LF are emitted at a backward angle α in the IF. (b) In the case when the angle between the polarization axis and the plane of the detector is 90°, all electrons emitted in the plane defined by the ion beam and the CEM_{90} detector have an emission angle $\theta = 90°$ with respect to the laser polarization in both reference frames, regardless of the angle α.

and $\psi = 90°$ in Eq. 2 we obtain

$$C_{\parallel} \propto 1 + \widetilde{\beta} P_2(1) = 1 + \widetilde{\beta},$$

and

$$C_{\perp} \propto 1 + \widetilde{\beta} P_2(0) = 1 - \frac{1}{2}\widetilde{\beta},$$

respectively. If we then define

$$\widetilde{Q} = \frac{C_{\perp}}{C_{\parallel}} \tag{3}$$

we get

$$\widetilde{\beta} = \frac{1 - \widetilde{Q}}{\widetilde{Q} + \frac{1}{2}}. \tag{4}$$

The $\widetilde{\beta}$ thus retrieved from the simulation can then be compared with the measured value.

3. Design of the spectrometer

PEARLS has been designed to study angular distributions of photoelectrons emitted from a linear source consisting of an ion beam collinearly interacting with a photon beam from a synchrotron radiation source. The extended collinear source enhances the rate of production of photoelectrons. To take advantage of the increased number of events one must be able to collect electrons along the extended source. **PEARLS** was designed for this purpose. The design also allows for the extraction of angular information without the need to rotate the polarization vector of the photons. A basic unit of **PEARLS** is a detector plane that is perpendicular to the ion/photon beams. It contains four Channel Electron Multipliers (CEMs) placed at $0°, 90°, 180°$ and $270°$ in the LF. Such a plane is shown in Fig. 2. The design incorporates four such detector planes in order to collect photoelectrons from an extended source length. Fig. 4 shows a cut-away drawing of **PEARLS**. The operational length of the linear source is defined by two adjacent graphite tubes with square cross sections. Each tube has a length of 11 cm and a 3 by 3 cm cross section. The graphite tubes are slightly separated to allow a scanner to be inserted to monitor the position of the ion beam. Graphite was chosen because it is known to have small patch fields on the surface [18]. Rows of small, equally-spaced holes are drilled on each of the four sides of the rectangular structure. These holes, numbering 14 on each side of a tube, allow the ejected electrons to exit the graphite tube and travel to a CEM. Electrons not passing through these holes will be absorbed by the graphite. Each tube is grounded to avoid charging by the absorbed electrons. Electrons exiting the holes pass through a filter consisting of a fine copper mesh. The filter can be biased to suppress low energy electrons. A copper plate is placed adjacent to the mesh and together they form a simple lens. After passing through the filter-lens combination, the electrons enter a rectangular copper box. These detector boxes, which are shown in Fig. 4, are divided into two by a copper wall. Each box contains a copper electrode, labeled U-plate in Fig. 4, that can be used to guide the electrons onto a CEM. The ion optics simulation program SIMION [19] has been used to simulate electron trajectories between the beam source and the CEMs. The design was optimized for transmission using a CEM front bias of +150V. Typical simulation patterns are shown in Fig. 5b, both with and without the central dividing wall. It can be seen that essentially all the electrons from the 14 holes can be collected if a central dividing wall is included in the design. A total of 8 CEMs are used to cover the four sides of each graphite tube. Therefore 16 CEMs are used to detect electrons from the two graphite tubes. These CEMs count photoelectrons emitted from about 22cm of the ion-photon beam source. Simulations show that approximately 4% of the electrons emitted from an isotropically distributed linear source are detected in **PEARLS**. This collection efficiency is considerably smaller than the 4π obtainable using a VMI spectrometer. However, the collinear beam interaction length of 22 cm used in the present **PEARLS** arrangement is some two orders of magnitude longer than a typical crossed beam source viewed in measurements made employing a VMI spectrometer. In addition, the beam interaction length

used in the present **PEARLS** arrangement, which is defined by four detection planes, can be easily increased by adding more detection planes. Furthermore, the electrons detected in a **PEARLS** measurement are emitted in a small range of angles around just two angles, $\theta = 0°$ and $\theta = 90°$. This is sufficient to determine the asymmetry parameter describing the photoelectron emission pattern (see Eq. 4). The combination of electron emission from a large source volume and the need to collect at only two angles, guarantees that the data acquisition time in a **PEARLS** experiment will be much shorter than an experiment involving a VMI spectrometer. In the future, electrostatic analyzers could be placed in front of each pair of CEMs if energy analysis of the photoelectrons were required. The geometry of such an arrangement is shown in Fig. 3. The chamber that houses the spectrometer has internal μ-metal shielding to reduce the effects of external magnetic fields on the photoelectron trajectories.

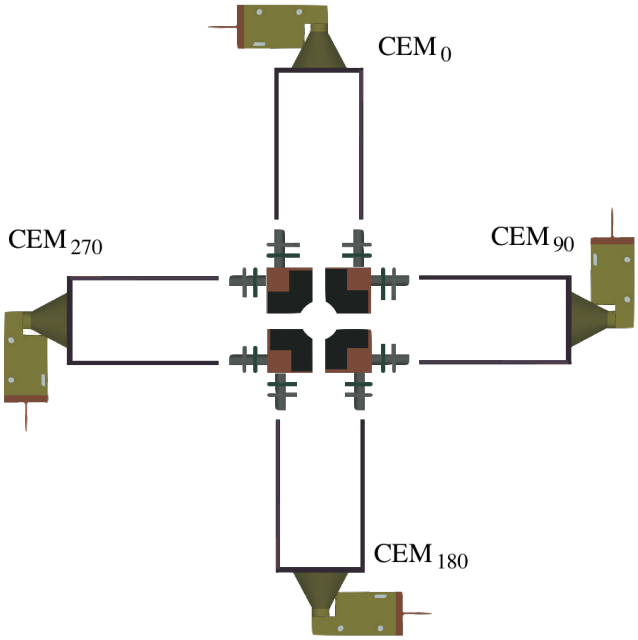

Figure 2: A schematic view of one of the four detector planes used in **PEARLS** as seen along the direction of propagation of the ion beam, which is directed into the paper. The four CEM:s are labeled by their spatial orientation in the laboratory.

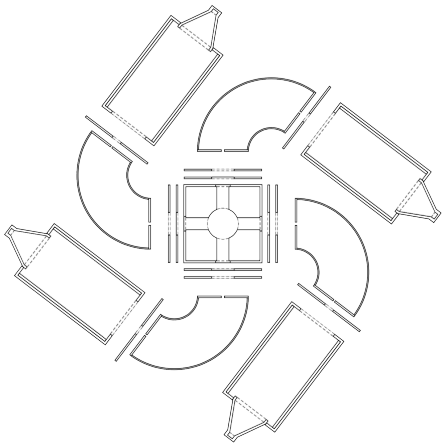

Figure 3: The figure shows the cross section of **PEARLS** when electrostatic analyzers have been added to the system (Compare with Fig. 2). The analyzers consist of cylindrical elements that extend along the whole length of the ion beam source viewed by **PEARLS**. It should be pointed out that these analyzers have not yet been installed at **PEARLS.**

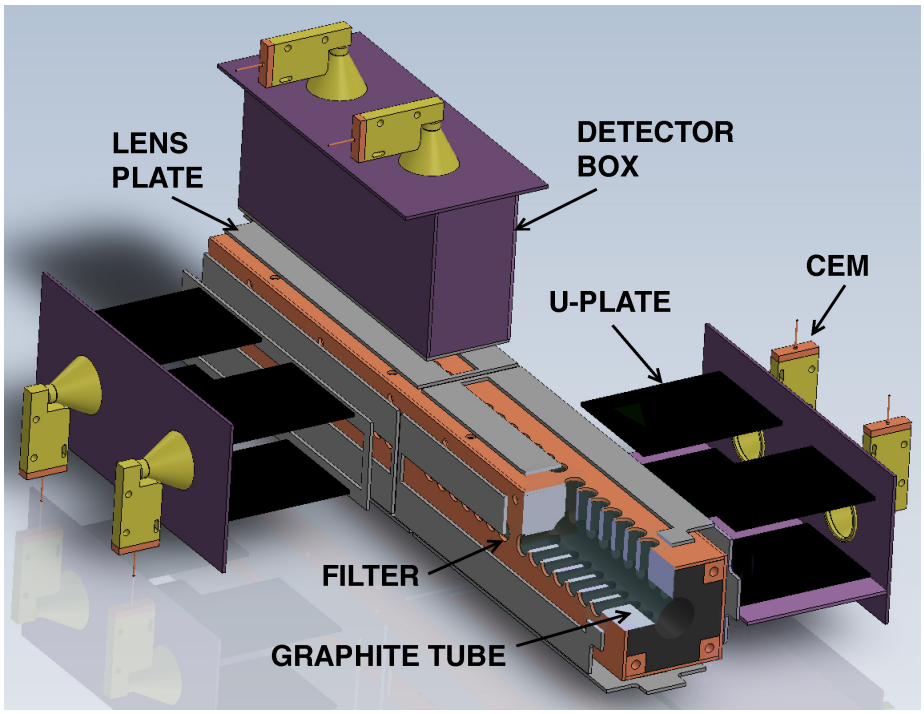

Figure 4: (Color online) A cut-away drawing of **PEARLS**. Selected components have been removed for clarity. 6 of the 16 symmetrically positioned CEMs are shown (yellow). The two graphite tubes are separated by a small gap. Detector boxes with U-plate electrodes are shown.

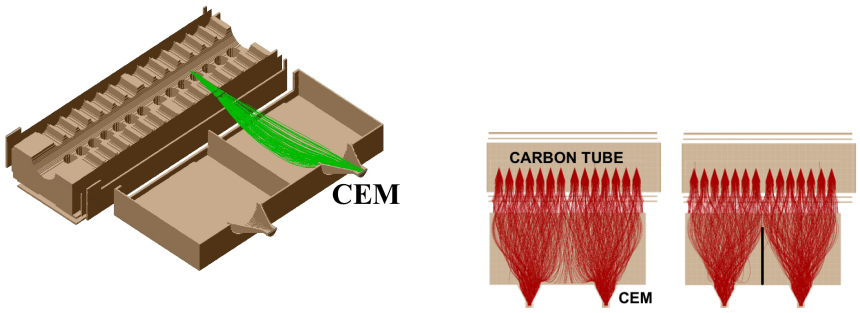

(a) (b)

Figure 5: (a) Cut-away of **PEARLS** showing SIMION simulations of the transmission and collection of electrons from the beam source to a CEM. In (b) the simulation shows the trajectories of electrons passing through all 14 holes in one of the graphite tubes. Electrodes in the detector box guide the electrons to one of the two CEMs. The simulation on the right demonstrates an improved collection if a dividing wall (black line) is used.

4. Tests of PEARLS using laser photodetachment

Due to the limited access to beamtime at synchrotron radiation sites, we conducted the initial tests and characterization of **PEARLS** at the **GUNILLA** (**G**othenburg **U**niversity **N**egative **I**on **L**aser **LA**boratory) facility using a laser as a photon source. In these test experiments, the angular distribution of electrons photodetached from a beam of Ag^- ions was studied at two photon energies in the visible. The bound electron in Ag^- occupies an s-orbital and so the detached electron in the final state will be represented by a pure p-wave. Within the dipole approximation, this case corresponds to an asymmetry parameter of $\beta = 2$, so the angular distribution is expected to have a $\cos^2\theta$ form, where θ is the angle between the linear polarization vector of the laser and the momentum vector of the detached electrons, as measured in the Ion Frame (IF). The **GUNILLA** apparatus has been described in detail elsewhere [20]. Fig. 6 is a schematic of the basic experimental arrangement used in the present work. Negative ions of Ag were produced in a sputter source, accelerated to a kinetic energy of 6 keV and focused into a beam using ion-optical elements. The ions were then mass selected using a 90° sector magnet. A number of additional ion-optical elements were used to optimize the transmission of the beam through **PEARLS**. **PEARLS** was located at the end of a 2 m long drift tube, along which the ion beam was overlapped with a laser beam entering the spectrometer in a direction opposite to that of the ion beam. The interaction region of the two counter-propagating beams within **PEARLS** was the source of the photodetached electrons. After the interaction region the ion beam was passed through a Quadrupole Deflector (QD), which was used to direct the remaining negative ions into a Faraday cup. The atoms in the beam, which arise primarily from photodetachment events, continued in the forward direction to a Neutral Particle Detector (NPD). This consisted of a tilted glass plate, where atoms that struck the plate produced secondary electrons that were counted by a CEM. The photon beam was produced by a Ti:Sapphire laser that was pumped by the frequency-doubled output of a Nd:YAG laser. The bandwidth was less than 6 GHz and the laser pulse duration in the order of 10-50 ns. A repetition rate of 5 kHz was used. The direction of the linear polarization vector of the laser could be rotated by use of a $\lambda/2$ Fresnel rhomb attached to a motorized rotation stage. The average power of the laser entering the vacuum chamber of **PEARLS** was around 50 mW. The amplified pulses from the CEMs used in **PEARLS** and the NPD were registered using time-gated counters. The counting channels were gated using the laser pulse as a trigger in order to enhance the signal-to-background ratio. The background, which arises primarily from the detachment in collisions of the negative ions with the residual gas in the apparatus, could be reduced to a negligible level by the use of narrow time gates. **PEARLS** was mounted in a vacuum chamber with a single turbo pump. Without baking, the chamber vacuum reached 10^{-8} mbar. The laser power and the ion current were simultaneously monitored and used for normalization in the data analysis.

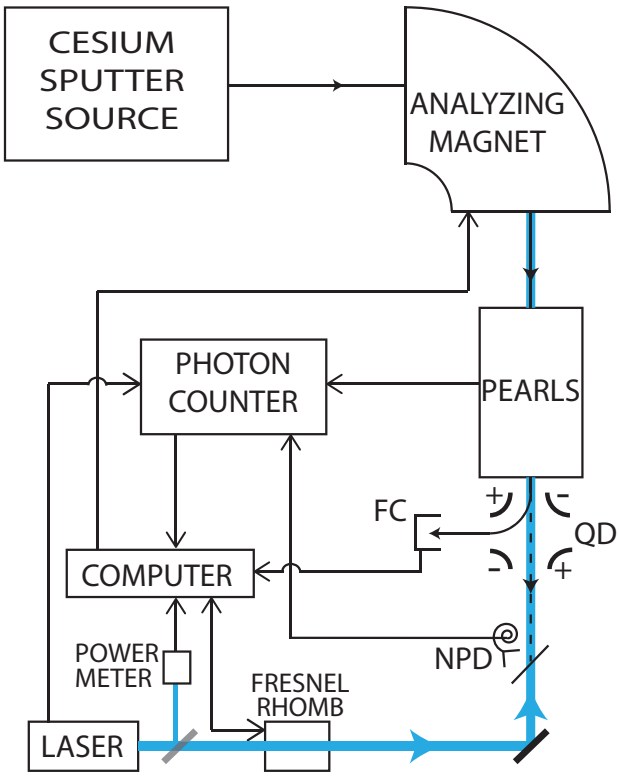

Figure 6: (Color online) A schematic of the experimental arrangement at **GUNILLA**. Negative ions are produced in a sputter source, accelerated and focused to form a unidirectional beam, mass selected by a magnet and passed through **PEARLS**. Inside **PEARLS** a linear source of photoelectrons is produced when the ions interact with a beam of laser light propagating in the opposite direction. A Quadrupole Deflector (QD) directs negative ions into a Faraday Cup (FC) and atoms are registered by a Neutral Particle Detector (NPD).

5. Results

In the test photodetachment experiments on Ag^-, the combination of a relatively large ion beam current and the high intensity and repetition rate of the laser provided us with a strong photoelectron signal. As a result, it was only necessary to use a single plane of four CEMs. In the experiment, photoelectrons were produced by photodetaching $^{109}Ag^-$ using the 405nm frequency-double output of the Ti:Sapphire laser. Fig. 7 shows the angular distribution curves as measured in each of the four CEMs. The angular step size was 10 degrees. The angle ψ that labels the horizontal axes refers to the orientation of the laser polarization vector in the laboratory frame, where $\psi = 0$ corresponds to a vertically-aligned polarization vector. All four curves shown in the figure exhibit a $\cos^2\theta$ angular distribution with θ being the angle between the laser polarization vector and the photoelectron momentum vector in the ion frame.

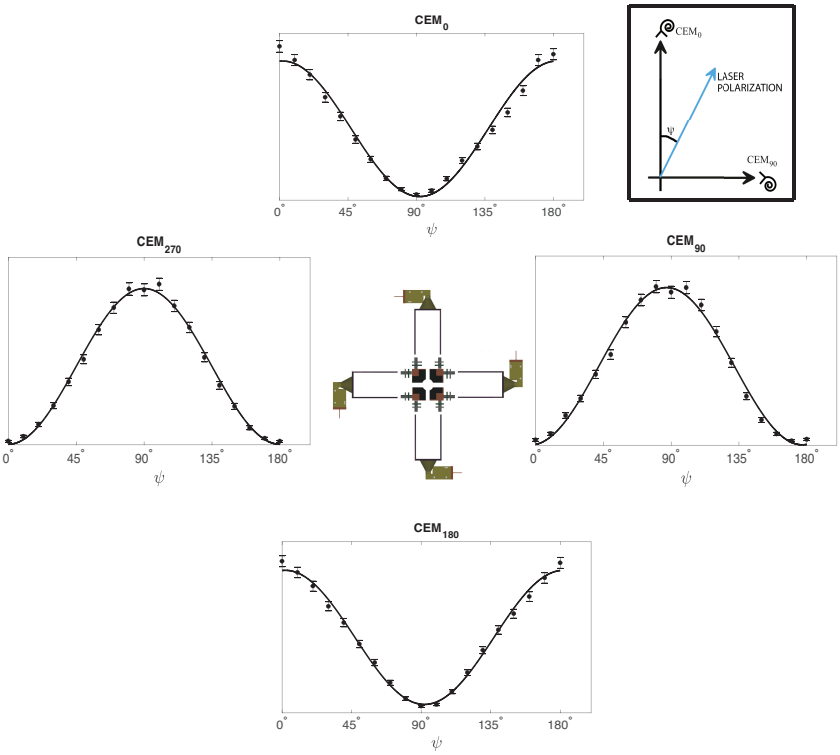

Figure 7: Angular distribution curves for the photoelectrons emitted in the photodetachment of Ag^- using a laser wavelength of 405nm. Each curve is associated with one of the 4 CEMs in a detector plane. The experimental data points show the normalized electron yields as a function of the angle ψ defined in the upper right. The solid lines are fits to Eq. 1.

A close inspection of the curves show that the yield at the minima are not exactly zero as expected for $\beta = 2$. This small discrepancy can be traced to a combination of two experimental artifacts. First, the finite size of the exit

holes in the graphite tube together with the extended source allow electrons within a range of emission angles to be detected by a CEM. This is purely a geometrical effect, as shown in Fig. 8a-b. Second, the velocity of the ions will cause the electron emission angles in the IF and LF to differ, as is described in detail in Sec. 2. This kinematic shift in emission angle between the two reference frames applies when the photoelectron emission angle $\theta \neq 90°$. In the data shown in Fig. 7 (Photodetachment of Ag^-, beam energy of 6 keV, wavelength 405 nm), the kinematic angle, defined as α in Fig. 1 is 7.5°. The combined effects of kinematics and the finite spread in acceptance angles of the spectrometer were studied by the use of a ray-tracing software, SIMION [19]. A cylindrical source of electrons was used in the simulation and the ion-frame emission angles followed a $\cos^2\theta$ distribution with respect to the polarization vector of the light. Fig. 8c-d shows a histogram from a SIMION simulation showing the angle between the detected electrons and the laser polarization when the detection direction is parallel (Fig. 8c) or perpendicular (Fig. 8d) with respect to the laser polarization.

The relative collection and detection efficiencies of the CEMs also need to be taken into consideration in the analysis of the data. The collection efficiencies could, for example, be slightly different if the laser-ion source were not exactly centered with respect to the four CEMs in the detector plane. In addition, the gain of the CEMs could be slightly different. By blocking the laser, one can observe electrons emitted from the ions when they collide with atoms/ions of the background gas. This isotropically-distributed background allowed us to adjust the experimental parameters in order to get an equal electron yield in all four CEMs.

Fig. 9 shows a comparison of the simulated data and the data obtained by measuring the angular distribution of electrons from the photodetachment of Ag^- using **PEARLS**. The experimental data points represent the combined yields from all four CEMs. The solid and dashed lines are fits to Eq. 1 for the experimental and simulated data, respectively. The fits produces values of the asymmetry parameter of $\beta^{exp} = 1.86 \pm 0.12$ and $\beta^{sim} = 1.96 \pm 0.06$. Hence, the experimental and simulated values agree within their uncertainties. Possible systemic effects that could affect the data will be discussed in Sec. 6.

Since **PEARLS** is designed to be used at a synchrotron radiation site without rotating the polarization vector of the light, a more realistic approach is to measure the yields $C_\parallel$ and $C_\perp$. By letting $C_\parallel = C_0 + C_{180}$ and $C_\perp = C_{90} + C_{270}$, it is straightforward to calculate $\widetilde{\beta}$ from Eq. 4. In the present work, we therefore adopted this procedure using the measured data shown in Fig. 7 at $\psi = 0$ and the $\widetilde{\beta}$ thus derived was compared with the simulation. We also used the 532nm pump beam of the Ti:Sapphire laser for a similar measurement. The results are shown in Tab. 1.

No energy analysis was needed in the test experiment since the emitted electrons were mono-energetic. We did, however, perform an additional photodetachment experiment, this time on $^{31}P^-$, in order to test the functionality of the energy filter that is incorporated into the design. The P^- ion was chosen

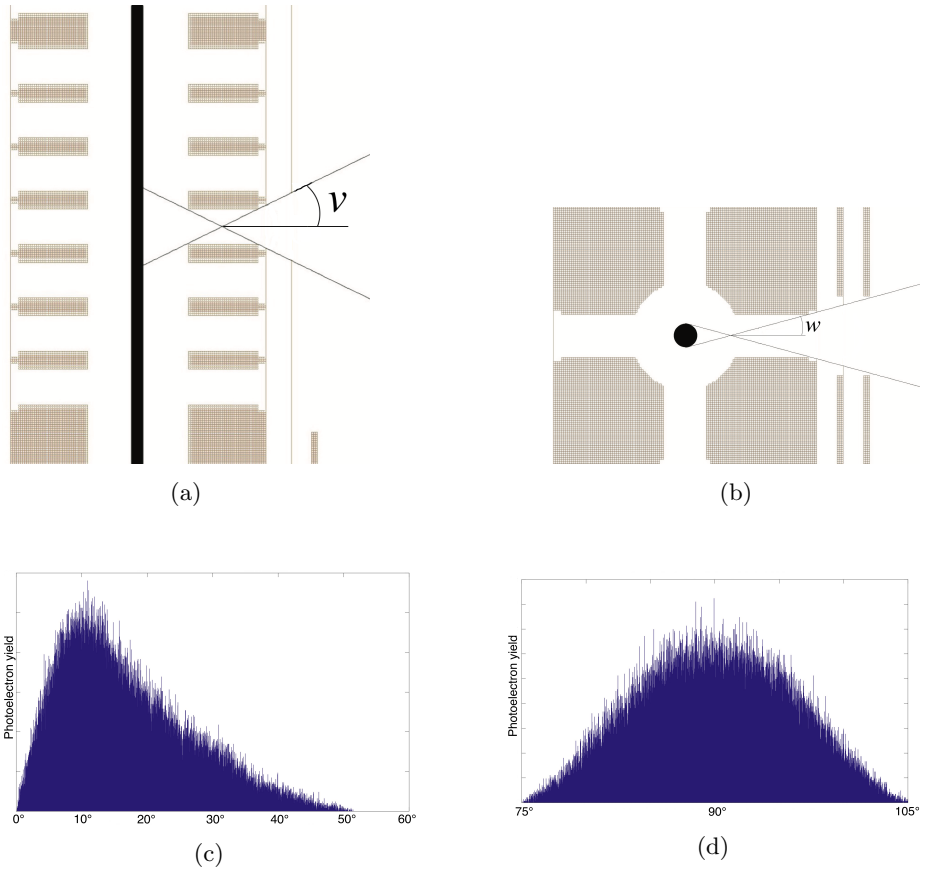

Figure 8: (a)-(b) The geometry of the interaction volume of **PEARLS** allows electrons within a range of angles with respect to the laser polarisation to escape the holes in the graphite tube and hence be detected. The black line (a) and circle (b) represent the merged ion and laser beams, respectively. The figures shows that the acceptance angle in the horizontal plane is larger than in the vertical direction, due to the linear nature of the collinear beam source. (c)-(d) Histogram from a SIMION simulation showing the IF angle between the momentum vectors of the detected electrons and the laser polarization when the detection direction in the LF is parallel (c) or perpendicular (d) with respect to the laser polarization.

because electrons of two different energies can be emitted in the photodetachment process via two open channels when using a photon energy of $E^f \approx 3.1$ eV. Fig. 10 shows two transitions in which the residual P atom is left in either the doublet $^2D_{3/2,5/2}$ state or the quartet $^4S_{3/2}$ state following photodetachment of P^-. The fine structure levels of the doublet P state are too close in energy to be resolved by the filter. Electrons emitted via these transitions will have energies of $E^{ex} \approx 0.95$ eV (excited level) and $E^0 \approx 2.35$ eV (ground level). An experiment was conducted to suppress the electrons using the simple high pass filter. Fig. 11 shows the normalized photoelectron yield in all four CEMs as a function of the filter voltage. The blue vertical line corresponds to the energy

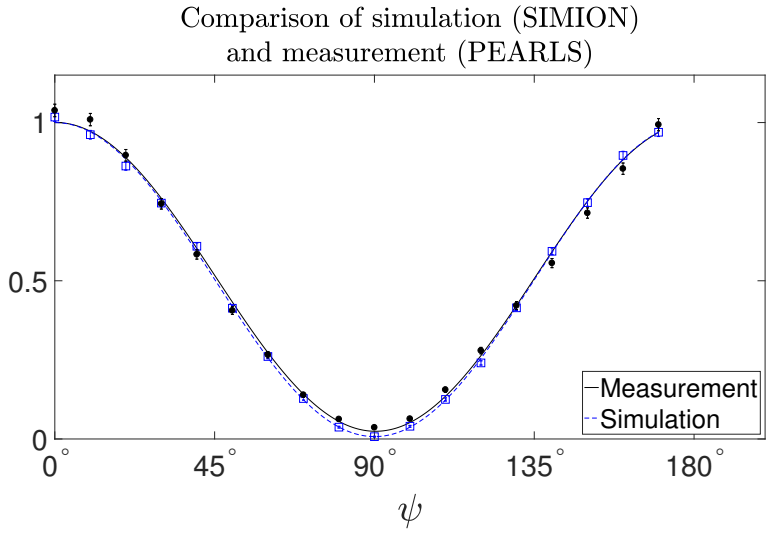

Figure 9: (Color online) The measured data (black dots) and the simulated data (blue squares) are shown together for comparison. The dashed blue line shows the fit to the simulated data. The solid black line shows the fit to the measured data from one of the CEMs in **PEARLS**.

Comparison of β for Ag^- at two different wavelengths.

λ (nm)	E_k (eV)	$\widetilde{\beta}_{fit}^{meas}$	$\widetilde{\beta}_{Q}^{meas}$	$\widetilde{\beta}_{fit}^{sim}$
405	1.76	1.86 ± 0.12	1.86 ± 0.11	1.96 ± 0.06
532	1.03		1.83 ± 0.09	1.95 ± 0.06

Table 1: The values $\widetilde{\beta}_{fit}$ correspond to the fitted functions in Fig. 9, while the values $\widetilde{\beta}_Q$ are calculated using Eq. 4 with yields from perpendicular pairs of CEMs at $\psi = 0°$ to emulate the situation in which the polarization vector of the light is fixed during a synchrotron-based measurement. E_k is the photoelectron energy. Errors for $\widetilde{\beta}$ are to one standard deviation.

286 E^{ex} of the excited state channel.

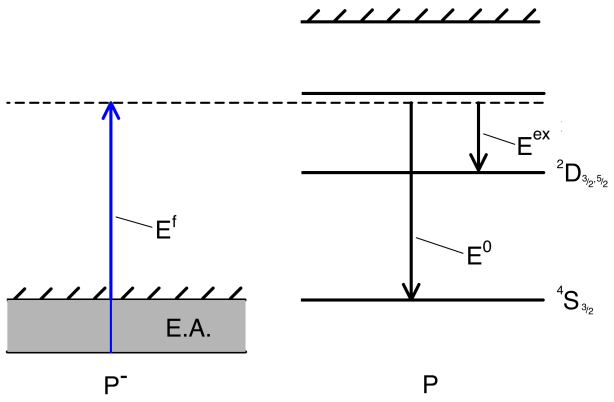

Figure 10: Partial energy level diagram showing two photodetachment transitions that leave the residual atom in the ground state and an excited state. Such transitions would produce photoelectrons at two different energies, $E^0 = E^f - E.A. \approx 2.35$ eV and $E^{ex} \approx 0.95$ eV [21, 22].

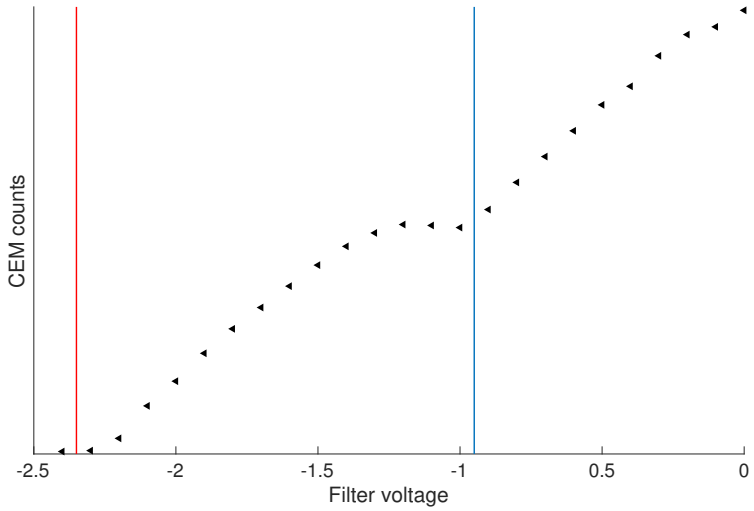

Figure 11: (Color online) Photoelectron yield as a function of filter voltage. It can be seen that electrons associated with the excited state transition with energy $E^{ex} \approx 0.95$ eV (vertical blue line) are fully suppressed when the filter voltage is set to -1V. The vertical red line corresponds to $E^0 \approx 2.35$ eV.

6. Discussion and conclusions

PEARLS was designed primarily to perform angular distribution measurements on photoelectrons emitted from a collinear source of interacting ions and synchrotron radiation. The design is based on the fact that the asymmetry parameter, β, which completely characterizes an angular distribution can, in principle, be determined by measuring the ratio of the electron yields in two detectors placed parallel and perpendicular with respect to a fixed polarization vector of the radiation. This mode of operation is necessary since rotation of the polarization of synchrotron radiation is difficult at most facilities. In order that such a measurement of an asymmetry parameter be successful, however, the two detectors must have the same counting efficiencies. One way to achieve this is to create an isotropic source of electrons. This can be achieved by blocking photons from the light source and detecting electrons emitted in collisions between the ions of the beam and atoms/molecules of the background gas. These collisionally detached electrons will be emitted isotropically with respect to the detector plane, i.e. the plane perpendicular to the direction of the ion beam. Such a procedure allows one to determine the relative counting efficiencies of the detectors and make suitable adjustments. Furthermore, the **PEARLS** design incorporates four detectors in each detector plane. Any pair of mutually orthogonal detectors should therefore give identical results, allowing one to adopt a normalization procedure to compensate for possible differences in counting efficiencies in the four detectors.

An investigation of the effects of kinematics and spread in acceptance angles due to the finite size of the exit holes in the graphite tubes has been made using ray-tracing simulations in SIMION. These simulations have allowed us to make a comparison of the measured and simulated data to account for the two effects mentioned above. Specifically, they have been applied to the data obtained in a test experiment involving the photodetachment of Ag^- using laser light. The angular distribution measurements yielded a value for the asymmetry parameter which was compared to a value obtained from a simulation that took into account the kinematic effect and the non-zero acceptance angle. Other systematic errors, where reflections of the electron on the graphite surfaces is estimated to be the most prominent [23], have not been included in the analysis. The value obtained from the simulation was in agreement with the measured value.

In the present paper, we performed a test measurement on an ion with known, constant asymmetry parameter. This choice made it a simple task to simulate the experiment using SIMION. A more realistic experimental situation, however, is to measure unknown asymmetry parameters. It is then possible to perform simulations that input electron distributions corresponding to different values of the asymmetry parameter β, and from these find a simulation for which $\widetilde{\beta}^{sim}$ agrees with the experimental result $\widetilde{\beta}^{exp}$.

An upgrade of **PEARLS** would make it possible to accommodate electrostatic energy analyzers in front of the CEMs. The ability to select electrons of different energies in future experiments would be a valuable asset. The present

design of **PEARLS** does, however, include a simple energy filter which we successfully tested in a separate experiment involving the photodetachment of P^-. In this case, electrons of two different energies were emitted. We were able to suppress the lower energy electrons of the bi-energetic pair.

Valuable information about the **PEARLS** apparatus has been obtained by substituting a laser for synchrotron radiation and performing a photodetachment experiment on a negative ion beam at the **GUNILLA** facility. The information thus obtained should be of value in future experiments at synchrotron sites. We are, for example, in the process of planning installations of **PEARLS**, initially at the ASTRID2 facility in Aarhus, and later at MAX IV in Lund. It should be pointed out that **PEARLS** was designed to be a general-purpose spectrometer, in that it could be used to perform angle-resolved measurements of the emission patterns of photoelectrons produced in the interaction of a beam of photons (synchrotron radiation, conventional lasers or free-electron lasers) with a beam of positive or negative ions of atoms, molecules, clusters or large biomolecules. We will initially use **PEARLS** to study angular distributions of electrons emitted in the photoionization of a beam of positive ions. Our first goal is to investigate the variation in the asymmetry parameter at energies around a "giant resonance" in the total photoionization cross section observed by West et al. [24] and investigated theoretically by Dolmatov et al. [25]. Another interesting application for **PEARLS** would be studying the angular pattern of photoelectrons emitted from ions of chiral molecules [9]

7. Acknowledgements

This work is supported by the Swedish Research Council. Financial support for the construction of **PEARLS** has been obtained from ALS and DOE. R.C. Bilodeau acknowledges funding from The Department of Energy, Office of Science, Basic Energy Sciences, Division of Chemical Sciences, Geosciences, and Biosciences under grant No. DE-SC0012376. The engineering work done by Bill Bates is also acknowledged.

[1] F Reinert and S Hufner. Photoemission spectroscopy - from early days to recent applications. *New Journal of Physics*, 7:34, 2005.

[2] T Andersen. Atomic negative ions: structure, dynamics and collisions. *Physics Reports-Review Section of Physics Letters*, 394(4-5):157–313, 2004.

[3] T Andersen, H K Haugen, and H Hotop. Binding energies in atomic negative ions: III. *Journal of Physical and Chemical Reference Data*, 28(6):1511–1533, 1999.

[4] R C Bilodeau and H K Haugen. Experimental studies of Os^-: Observation of a bound-bound electric dipole transition in an atomic negative ion. *Physical Review Letters*, 85(3):534–537, 2000.

[5] C. W. Walter, N. D. Gibson, D. J. Matyas, C. Crocker, K. A. Dungan, B. R. Matola, and J. Rohlén. Candidate for laser cooling of a negative ion: Observations of bound-bound transitions in La^-. *Physical Review Letters*, 113(6), 2014.

[6] J C Rienstra-Kiracofe, G S Tschumper, H F Schaefer, S Nandi, and G B Ellison. Atomic and molecular electron affinities: Photoelectron experiments and theoretical computations. *Chemical Reviews*, 102(1):231–282, 2002.

[7] G Aravind, A K Gupta, M Krishnamurthy, and E Krishnakumar. Photodetachment studies with the linear time of flight photoelectron spectrometer. *Journal of Physics: Conference Series*, 80(1):012026, 9 2007.

[8] J. Cooper and R. N. Zare. Angular Distribution of Photoelectrons. *The Journal of Chemical Physics*, 48(2):942–943, 1 1968.

[9] Katharine L Reid. Photoelectron angular distributions. *Annual review of physical chemistry*, 54(19):397–424, 2003.

[10] C. Domesle, B. Jordon-Thaden, L. Lammich, M. Förstel, U. Hergenhahn, A. Wolf, and H. B. Pedersen. Photoelectron spectroscopy of O^- at 266 nm: Ratio of ground- and excited-state atomic oxygen production and channel-resolved photoelectron anisotropy parameters. *Physical Review A - Atomic, Molecular, and Optical Physics*, 82(3):033402, 9 2010.

[11] H Kjeldsen, P Andersen, F Folkmann, B Kristensen, and T Andersen. Inner-shell photodetachment of Li^-. *Journal of Physics B: Atomic, Molecular and Optical Physics*, 34(10):L353–L357, 5 2001.

[12] D J Pegg, C Y Tang, J Dellwo, and G D Alton. Angular distribution of electrons photodetached from the excited negative ion of carbon. *Journal of Physics B-Atomic Molecular and Optical Physics*, 26(22):L789–L792, 1993.

[13] Hannes Hultgren, Mikael Eklund, Dag Hanstorp, and Igor Yu. Kiyan. Electron dynamics in the ground state of a laser-generated carbon atom. *Physical Review A*, 87(3):031404, 3 2013.

[14] D Hanstorp. An ion beam apparatus for collinear photodetachment experiments. *Nuclear Instruments & Methods in Physics Research Section B-Beam Interactions with Materials and Atoms*, 100(1):165–175, 1995.

[15] D Hanstorp, C Bengtsson, and D J Larson. Angular distributions in photodetachment from O^-. *Physical Review A*, 40(2):670–675, 1989.

[16] B Rouvellou, J M Bizau, D Cubaynes, L Journel, S AlMoussalami, and F J Wuilleumier. A dedicated electron spectrometer for photoionization studies of atomic ions with synchrotron radiation. *Journal of Electron Spectroscopy and Related Phenomena*, 76:237–243, 1995.

[17] S AlMoussalami, J M Bizau, B Rouvellou, D Cubaynes, L Journel, F J Wuilleumier, J Obert, J C Putaux, T J Morgan, and M Richter. First angle-resolved photoelectron measurements following inner-shell resonant excitation in a singly charged ion. *Physical Review Letters*, 76(24):4496–4499, 1996.

[18] Russell D. Young and Howard E. Clark. Effect of Surface Patch Fields on Field-Emission Work-Function Determinations. *Physical Review Letters*, 17(7):351–353, 8 1966.

[19] Scientific Instrument Services Inc. (www.simion.com). SIMION v8.1.

[20] C Diehl, K Wendt, A O Lindahl, P Andersson, and D Hanstorp. Ion optical design of a collinear laser-negative ion beam apparatus. *Review of Scientific Instruments*, 82(5):7, 2011.

[21] W. C. Martin, Romuald Zalubas, and Arlene Musgrove. Energy Levels of Phosphorus, P i through P xv. *Journal of Physical and Chemical Reference Data*, 14(3):751–802, 1985.

[22] R J Peláez, C Blondel, M Vandevraye, C Drag, and C Delsart. Photodetachment microscopy to an excited spectral term and the electron affinity of phosphorus. *J. Phys. B: At. Mol. Opt. Phys.*, 44(19):195009, 2011.

[23] D Hanstorp, M Gustafsson, U Berzinsh, and U Ljungblad. Collinear photodetachment spectroscopy. *Nuclear Instruments & Methods in Physics Research Section B-Beam Interactions with Materials and Atoms*, 79(1-4):159–161, 1993.

[24] J. B. West, J. E. Hansen, B. Kristensen, F. Folkmann, and H. Kjeldsen. Revised interpretation of the photoionization of Cr^+ in the 3p excitation region. *J. Phys. B: At. Mol. Opt. Phys.*, 36:L327–L333, 2003.

[25] V. K. Dolmatov, E. Guler, and S. T. Manson. "Reading" the Photoelectron β-Parameter Spectrum in a Resonance Region. *Physical Review A - Atomic, Molecular, and Optical Physics*, 76(3):2–6, 2007.